Nov 6th, 12:00 AM - 12:00 AM

Towards Load-Deformation Models for Screw-Fastened Cold-Formed Steel-to-Steel Shear Connections

C. D. Moen

D. A. Padilla-Llano

S. Corner

C. Ding

Twenty-Second International Specialty Conference on Cold-Formed Steel Structures
St. Louis, Missouri, USA, November 5 & 6, 2014

Towards Load-Deformation Models for Screw-Fastened Cold-Formed Steel-to-Steel Shear Connections

C.D. Moen[1], D. A. Padilla-Llano [2], S. Corner[3], C. Ding[4]

Abstract

This paper summarizes results from an experimental program considering single-fastened cold-formed steel-to-steel shear connections. Fastener motion (displacement and tilting angle) and bearing deformation occurring on the connecting members at the fastener location were captured using an automated, optical non-contact measurement procedure. The results are used to relate cold-formed steel-to-steel shear connection load-deformation response to tilting and bearing response. A general steel-to-steel single shear fastener load-deformation equation is also proposed and demonstrated.

Introduction

Steel-to-steel screw through-fastened connections are a staple of light steel framed construction. There are thousands of screw fasteners in a light steel-framed building – connecting studs to tracks, forming strap braced and sheathed shear walls, and attaching gypsum to interior partitions. Considered together, these components and their connections define building system behavior - especially lateral drift and seismic performance as demonstrated by recent full scale building tests (Leng et al. 2012). The goal of this paper is to lay the groundwork for mechanics-based screw fastener load-deformation models. These forthcoming models will have wide applicability – serving as input to 3D building system modeling and providing equations for code-based sheathing-to-member (stud, joist) deformation compatibility checks.

Screw fasteners are easy to install but their stiffness and strength contributions to the structural system are exceedingly difficult to quantify because of complex

[1] Associate Professor, Virginia Tech, cmoen@vt.edu
[2] Graduate Research Assistant, Virginia Tech, dapadill@vt.edu
[3] Graduate Research Assistant, Virginia Tech, scorner@vt.edu
[4] Graduate Research Assistant, Virginia Tech, chud91@vt.edu

kinematics, for example, screw head contact and screw-thread interaction. Recent research demonstrates that if cyclic fastener stiffness and strength degradation is carefully documented with tests and then modeled, for example with the commonly applied OpenSees Pinching4 material model (McKenna et al. 2000), sheathed cold-formed steel shear wall and diaphragm behavior can be directly simulated, without empirical treatments (Buonopane et al. 2014; Chatterjee et al. 2014).

Connection capacity is the focus of most cold-formed steel connection experimental programs in the literature, which is perfectly reasonable for the component level load and resistance factor approaches currently employed in design. A shift to system design is occurring however, which requires not only capacity but also stiffness and stiffness degradation with varying load. The focus of the work presented herein is to study individual steel-to-steel fastener connections and their full load-deformation response, including stiffness degradation as the connection progresses through tilting, bearing, and tearing, with the goal of identifying key kinematics that will lead to response equations for enabling future light steel framing system design.

This paper documents an experimental program on single steel-to-steel through-fastened screw connections. The trends discussed herein are taken from subset of over 200 monotonic connection tests are conducted with varying t_2/t_1 ply thickness combinations, screw sizes (#8, #10, #12), and configurations (web to web, flange to web, sheet to sheet) that will be fully documented in an upcoming AISI report. Optical non-contact measurement techniques allow for fastener tracking – screw rotation and translation, up to and beyond peak load. The tracking information provides quantitative correlation between fastener and ply deformation and stiffness degradation that inspires load-deformation equations proposed at the end of the paper. The next section provides more background on cold-formed steel connections pertinent to fastener stiffness and strength.

Cold-formed steel connections: background and behavior

Cold-formed steel-to-steel connection tested behavior, both bolted and screw-fastened, are thoroughly documented in the literature. Bolted connected strength limit states are defined by tearing along planes parallel to bolt shear for thin sheet plies, also inclined tearing with material piling up in front of the bolt, transitioning to transverse tearing at the bolt bearing point and then screw shear as ply thickness increases (Winter 1956; Zadanfarrokh and Bryan 1992). Cold-formed steel connection stiffness research resides primarily in bolted connections to improve cold-formed steel truss modeling (Zaharia and Dubina

2006) where both axial and flexural stiffness are empirically derived from tests, and for bolted moment frames (Lim and Nethercot 2004; Uang et al. 2010) where connection strength and stiffness are important for predicting wind and seismic drift.

The current AISI steel-to-steel screw fastened capacity prediction equations (AISI 2012, Section E4.3) for tilting, bearing, and screw shear limit states were developed by modifying existing equations (ECCS 1987; British Standards Institution 1987), most notably a change from ply yield strength to ultimate tensile strength that resulted in better predictions confirmed with a compilation study of over 3,500 tests (Peköz 1990; van der Merwe 1987). Strain hardened steels from cold-forming increase fastener capacity and change fastener load-deformation and limit states, for example tearing for high ductility steels may be supplanted by tilting and bearing when the steel thickness is cold-reduced (Daudet and LaBoube 1996).

Screw tilting and bearing strength limit states are defined in the AISI specification based on the plate thickness ratio t_1/t_2, where t_1 is the base metal thickness for the sheet ply in contact with the fastener head and t_2 is the base metal thickness of the adjacent ply typically embedded with at least one fastener thread. Most of these tests were performed by pulling on thin eccentric steel plates, artificially amplifies the tilting and rotation when compared to a typical stud-to-stud or stud-to-track connection which complicates limit state predictions, especially screw shear (Serrette and Peyton 2009).

The tilting limit state is assumed to occur in the AISI capacity equations when $t_2/t_1 \leqslant 1.0$. Tilting occurs because the force couple resisted by the plies, resulting from the moment in an eccentric single shear connection, causes the fastener hole to elongate in the t_2 ply. As the t_2 ply thickness decreases, the moment arm reduces and the force couple magnitude increases. A tilting failure occurs when a screw, inclined at an angle because of the moment and associated rotation caused by the force eccentricity in the connection, pulls through the t_2 ply.

A bearing failure occurs when the concentrated pressure from the fastener on the t_1 or t_2 plies exceeds the steel yield stress causing hole elongation at a constant bearing stress, i.e., the connection shear stiffness decreases to zero. The bearing stress magnitude that causes the stiffness loss varies with fastener distance to an edge. More plate material behind the fastener increases the bearing failure pressure, a phenomenon first documented in bolted cold-formed steel connections (Winter 1956). In the study summarized herein, edge distance on the order of 10 times the fastener diameter is provided and is therefore not a variable.

For thicker plies (97 mils or 2.5 mm) local buckling deformation is minimal in front of a hole and the force can spread and redistribute in the plies. However for thinner plies (33 mils or 0.9 mm) local buckling decreases the ply resistance to bearing. In this case the bearing force is distributed with a tension tie; if the stress in this tension tie exceed the steel ultimate stress, the steel 'rips' in front of the fastener. If both plies are sufficiently thick, then the connection can carry the fastener's shear capacity which is typically determined by each screw manufacturer.

Recent studies show that increasing the number of screws in a connection reduces the strength per screw (Laboube and Sokol 2002). This phenomenon is well documented in reliability theory for a parallel ductile system where the element with the lowest strength redistributes load to its neighbors, driving the system failure (Hendawi and Frangopol 1994). Tests studying combined strength limit states, for example, connections under tension pullout and shear (Francka and LaBoube 2009) demonstrated that screw fastened connection under tension and shear typically failed in a combination of screw pull-out, tilting and sheet bearing. Screw fastened connections can experience multiple strength limit states at once (Casafont et al. 2006), for example tilting and net section failure and tilting, bearing, and pullout. For simplicity and to concentrate on limit state correlation to load-deformation response, only one fastener is considered in the following test program.

Experimental program

This experimental program focuses on load-deformation response of screw-fastened cold-formed steel steel-to-steel shear connections. The test setup employs sheet-to-sheet boundary conditions shown in Figure 1. Custom machined test figures and a screw driven MTS testing machine were used to perform the monotonic tests as illustrated in Figure 1. A 150 kN load cell measured applied force and cross head displacement was recorded with an internal LVDT with an accuracy of $\pm$ 0.01 mm. A single #10 hex-washer head self-drilling screw (Simpson Strong-Tie X-Screw series, 4.82 mm diameter with thread) is centered in the 102 mm by 102 mm sheet window for all tests. The crosshead loading rate is 0.025 mm/sec.

Testing strategy

The steel-to-steel screw through-fastened connection test matrix is summarized in Table 1. Base metal ply thickness combinations were selected to isolate AISI tilting, tilting plus bearing, and bearing conditions, and three monotonic tests per permutation were performed (except for the 6843 series). The specimen naming

notation defines ply 1 and 2 thicknesses in mils (33, 43, 68, and 97) and test number. For example, 3333-1 defines ply 1 and ply 2 as 33 and 33 mils and the test number 1 of 3.

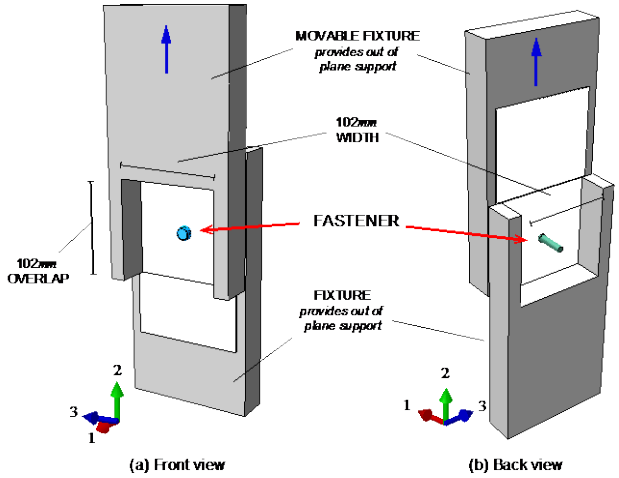

Figure 1. Test setup with sheet style boundary conditions where two machined aluminum parts (one bolted to the cross head, one bolted to the testing machine base) creates a 102 by 102 mm square testing area. This setup eliminates specimen curling caused by the moment in the single shear connection.

Table 1. Test matrix, measured base metal ply thicknesses t_1 and t_2, yield stress F_y and ultimate stress F_u from tensile coupons

Specimen	t_1 [mm]	t_2 [mm]	F_{u1} [MPa]	F_{y1} [MPa]	F_{u2} [MPa]	F_{y2} [MPa]
3333-1	0.880	0.880	446	333	446	333
3333-2	0.871	0.871	444	334	444	334
3333-3	0.871	0.871	444	334	444	334
4343-1	1.188	1.188	456	337	456	337
4343-2	1.189	1.189	455	338	455	338
4343-3	1.189	1.189	455	338	455	338
6843-1	1.812	1.187	496	392	456	338
6843-2	1.812	1.187	496	392	456	338
4368-1	1.187	1.828	456	338	492	376
4368-2	1.187	1.828	456	338	492	376
4368-3	1.187	1.828	456	338	492	376
9797-1	2.553	2.553	523	402	523	402
9797-2	2.553	2.553	523	402	523	402
9797-3	2.553	2.553	523	402	523	402

Ply material properties and base metal thickness

Web base metal thickness t_1 and t_2 (i.e., thickness with zinc coating removed) yield stress, F_y, and ultimate strength F_u, were measured for plies 1 and 2 in each specimen. These values are reported in Table 1 as an average of two tensile coupons per sheet measured in accordance with ASTM E8M-08 (ASTM 2008).

Tilting and relative displacement measurements using optical techniques

Fastener rotation and translation were tracked with a custom optical non-contact measurement system (Figure 2a). A rod with two colored circular targets was glued at three locations on a specimen – (*i*) on the fastener head, (*ii*) at 114 mm (4.5 in.) up from the Ply 1 edge, and (*iii*) 25.4 mm (1 in.) down from the Ply 2 edge. The change in vertical displacement between (ii) and (iii) is defined as the ply relative displacement, δ.

Target motion is captured at 1 frame per second with a 35 mm digital SLR camera and then post-processed using Matlab's image processing toolbox to track the movement of the colored targets. For example, the fastener target (*i*) coordinates (C_x, C_y) and (c_x, c_y) as shown in Figure 2b are determined in each picture frame and used to calculate the fastener head rotation θ and translation ($X_f - X_0$, $Y_f - Y_0$). Rod length measurements (L_{rod}) were carefully recorded before each test. Optical measurement accuracy is ±0.05 mm (Haus 2013).

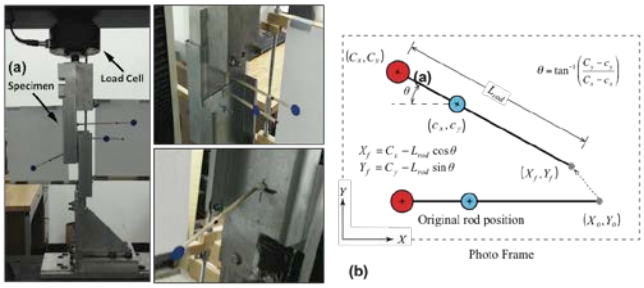

Figure 2. Optical relative ply displacement (δ) and screw tilting angle (θ) measurements: (a) optical markers and test setup; (b) screw tracking geometry for fastener target (*i*)

Test Results and Observations

Screw fastened connection load-deformation response is summarized in Figure 3, where the load is the applied load to Ply 1 (P) and the deformation is the relative displacement between plies (δ) measured with the optical techniques described previously. As expected, the 3333 specimens are tilting dominated consistent with AISI S100-12 Section E4 screw fastened limit state equations.

The average tilting angle θ=22 degrees at peak load P_{test}=2780 N (again an average of three tests) as shown in Table 2. Note that the connection capacity P_{test} is defined for each test as the first maximum peak load after softening.

The increased ply thickness in the 4343 tests has a minimal effect on tilting deformation, compare θ=19 degrees to θ=22 degrees for the 3333 tests. The increased thickness does boost connection capacity by 75% however to P_{test}=4845 N when compared to the 3333 tests. The fastener finds more moment resistance as it tilts through Ply 2. The higher capacity comes from the added t_2 bearing strength that is predicted to increase by 65% when going from 33 to 43 mils in AISI S100-12 Equation E4.3.1-5. Screw shear dominates in the 9797 tests with minimal tilting (θ=1.7 degrees on average) which is consistent with AISI predictions.

The 6843 specimens exhibit less tilting than the 3333 and 4343 tests, with the average θ=6 degrees at P_{test}=6608 N. Fastener tilting is limited by the 68 mil Ply 1 which prevents head rotation. Also the moment arm on the fastener increases (68/2+43/2 instead of 33/2+33/2 for example) reducing bearing demand from tilting on both Ply 1 and Ply 2. The moment concentrates at the Ply 1 head contact because its stiffness is higher than the 43 Ply 2, causing a brittle failure at peak load as the fastener shaft breaks at the screw head, see Figure 3d.

The 4368 fastener rotation increases to θ=10 degrees on average (from θ=6 degrees for the 6843) because the fastener head is not as well restrained by the 43 mil Ply 1. Average connection capacity is similar to the 6843 tests, with P_{test}=6285 N. The failure mode is notably different in the 4368 tests however, with post peak hardening resulting from bearing and material piling in the 68 mil Ply 2. The fastener is restricted until it starts pulling out in a combined tension-shear mode, with each load-deformation undulation in Figure 3e caused by a thread pulling through Ply 2.

The AISI S100-12 Section E4 fastener capacity P_{ns} for all tests are summarized along with the governing limit state equation in Table 3. Test-to-predicted mean and COV are 0.90 and 0.17 respectively. The AISI equations underpredict capacity for both bearing and tilting behavior, which is consistent with other recent test programs (e.g., Serrette and Peyton 2009). The 9797 ‘shear failure’ capacities are also lower than the manufacturer screw shear capacity (P_{ss} in AISI S100-12). It is hypothesized that the lower shear strength is caused by combined screw shear and bending in the 9797 tests which does not occur in manufacturer tests where the ply thicknesses are higher, typically 6.3 mm for Plies 1 and 2.

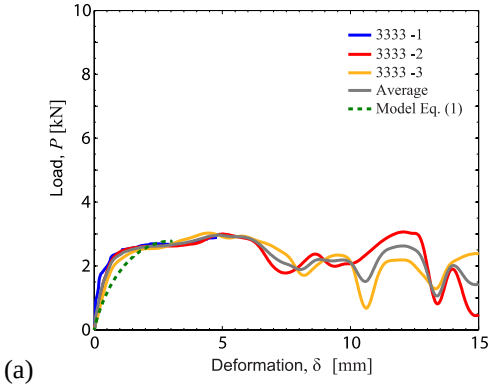
3333 -1
3333 -2
3333 -3
Average
Model Eq. (1)
Load, P [kN]
Deformation, δ [mm]
0
2
4
6
8
10
0
5
10
15

(a)

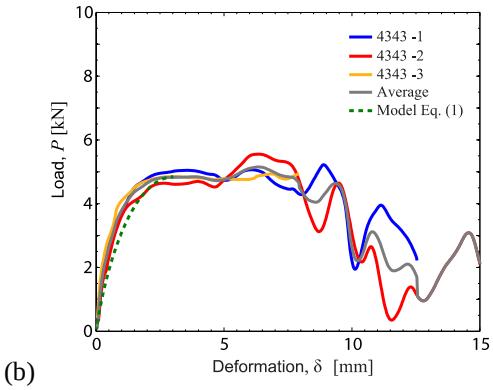
4343 -1
4343 -2
4343 -3
Average
Model Eq. (1)
Load, P [kN]
Deformation, δ [mm]
0
2
4
6
8
10
0
5
10
15

(b)

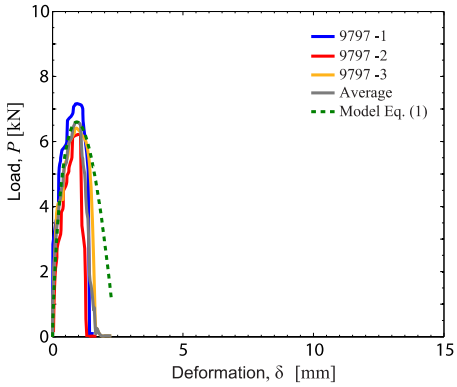
9797 -1
9797 -2
9797 -3
Average
Model Eq. (1)
Load, P [kN]
Deformation, δ [mm]
0
2
4
6
8
10
0
5
10
15

(c)

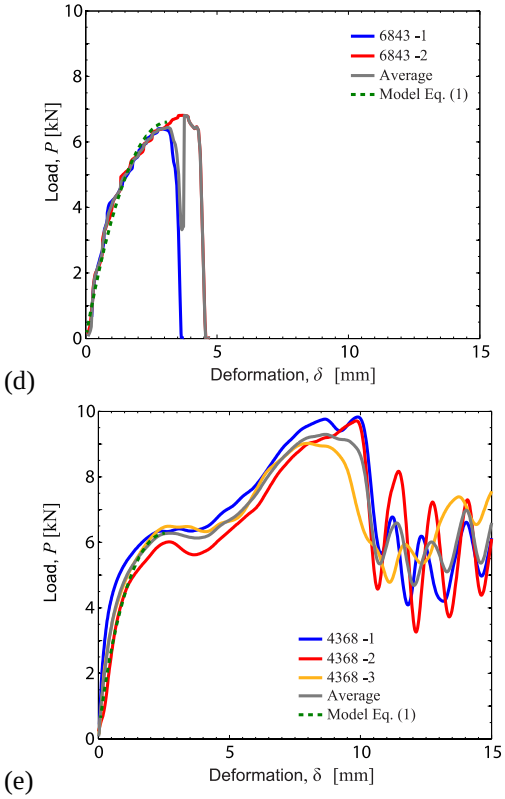

Figure 3. Screw fastener load versus relative ply displacement for: (a) 3333; (b) 4343; (c) 9797; (d) 6843; and (e) 4368 test groups.

Table 2. Test results and AISI limit state predictions (See AISI-S100-12 for limit state equations)

Specimen	P_{test} [N]	P_{ns} [N]	P_{test}/P_{ns}	AISI Limit State	δ_{test} [mm]	θ_{test} [degrees]	k_o [N/mm]
3333-1	2695	3395	0.79	E4.3.1-1	2.30	21	11420
3333-2	2615	3330	0.78	E4.3.1-1	2.40	17	4150
3333-3	3030	3330	0.91	E4.3.1-1	4.50	27	3150
Average	2780	3352	0.83	-	3.07	21.7	6240
COV	0.08	0.01	0.08	-	0.41	0.23	0.72
4343-1	5045	5450	0.93	E4.3.1-1	3.55	22	6490
4343-2	4645	5445	0.85	E4.3.1-1	2.55	17	5600
4343-3	4850	5445	0.89	E4.3.1-1	3.10	18	9530
Average	4847	5447	0.89	-	3.07	19.0	7207
COV	0.04	0.00	0.04	-	0.16	0.14	0.29
6843-1	6405	5445	1.18	E4.3.1-1	2.60	9	4690
6843-2	6810	5445	1.25	E4.3.1-1	3.65	10	4420
Average	6608	5445	1.21	-	3.13	9.5	4555
COV	0.04	0.00	0.04	-	0.24	0.07	0.04
4368-1	6345	7055	0.90	E4.3.1-2/4	2.35	12	14510
4368-2	6015	7055	0.85	E4.3.1-2/4	2.70	15	4740
4368-3	6495	7055	0.92	E4.3.1-2/4	2.70	15	8790
Average	6285	7055	0.89	-	2.58	14.0	9347
COV	0.04	0.00	0.04	-	0.08	0.12	0.53
9797-1	7170	8160	0.88	E4.3.3	0.95	2	162370
9797-2	6215	8160	0.76	E4.3.3	0.95	1	16160
9797-3	6415	8160	0.79	E4.3.3	0.90	2	40380
Average	6600	8160	0.81	-	0.93	1.7	72970
COV	0.08	0.00	0.08	-	0.03	0.35	1.07

Proposed Load-Deformation Model

The test observations lead to the following proposed load-deformation generalization shown in Figure 4, with the defining equations as

$$P(\delta) = k_o\left(\delta - \gamma\delta_f\left(\frac{\delta}{\delta_f}\right)^{\frac{1}{\gamma}}\right),\ \gamma = 1 - \left(\frac{P_f}{k_o\delta_f}\right) \qquad (1)$$

where P_f is the fastener peak load, $\delta_{\square}$ is the relative ply displacement at peak load, and k_o is the initial tangent stiffness. The model viability is demonstrated in Figure 3, compare the 'model' and 'average' curves where $P_f = P_{test}$, $\delta_{\square} = \delta_{test}$, and k_o is calculated using the 'average' curve linear regression slope from the origin to $0.4P_{test}$ (see Table 2). With more research and validation it is envisioned that AISI Section E4 prediction equations can be used to calculated P_f. Mechanics-based models for calculating k_o and $\delta_{\square}$ considering plate and bearing stiffness are currently under development. Equation modifications to capture post-peak behavior (ductile hardening or brittle failure) are also being considered.

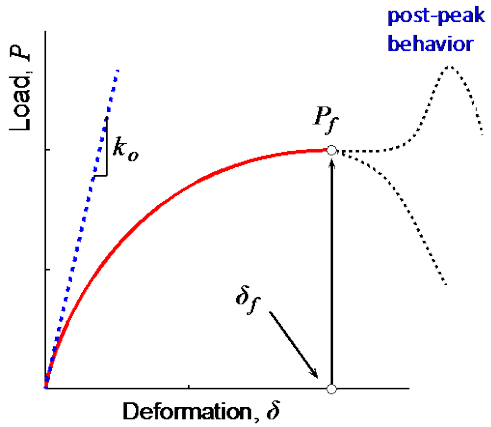

Figure 4. Steel-to-steel single shear screw connection load-deformation model

Conclusion

Cold-formed steel-to-steel through-fastened screw connections were performed to correlate existing tilting, bearing, and shear limit states to single fastener load-deformation response. Optical methods measured relative ply displacement and tracked fastener tilting angle. Tilting dominated for thin plies, transitioning to bearing and then to screw shear as ply thickness increased. When the thicker ply was in contact with the screw head, tilting rotation was restrained which caused screw bending and brittle screw fracture. When the thicker steel sheet ply contains the fastener tip, tilting deformation results in a ductile bearing mode with post-peak hardening. AISI fastener strength predictions were on average higher than the tested values. A general fastener load-deformation model was proposed, and work is ongoing to fully develop it parameters and applicability in light steel framing system design and analysis.

Acknowledgements

The authors are grateful for the steel and fastener donations obtained through Greg Ralph at Clark Dietrich Building Systems and Randy Daudet from Simpson Strong Tie. The authors received thoughtful guidance from the AISI project monitoring task group “Energy Dissipation of Cold-Formed Steel Connections”, with special thanks to Bonnie Manley, Jay Larson, Ben Schafer, Bill Gould, Cheng Yu, Chia-Ming Uang, and Steve Tipping. Virginia Tech undergraduate researchers Heather Todak and Justin White contributed to the connection testing.

References

AISI (2012). "North American specification for the design of cold-formed steel structural members." Section E.4.3, American Iron and Steel Institute, Washington , D.C.

BSI (1987). "British Standard - Structural Use of Steelwork in Building - Part 5. Code of Practice for Design of Cold-Formed Sections."

Buonopane, S. G., Tun, T. H., and Schafer, B. W. (2014). "Fastener-based computational models for prediction of seismic behavior of CFS shear walls." Tenth U.S. National Conference on Earthquake Engineering Frontiers of Earthquake EngineeringAnchorage, Alaska, U.S.A.

Casafont, M., Arnedo, A., Roure, F., and Rodrı´guez-Ferran, A. (2006). "Experimental testing of joints for seismic design of lightweight structures. Part 1. Screwed joints in straps." Thin-Walled Structrures, 44(2), 197–210.

Chatterjee, A., Moen, C. D., Arwade, S. R., and Schafer, B. W. (2014). "System reliability sensitivity to fastener capacity in cold-formed steel wood-sheathed floor diaphragms." Proc., EUROSTEEL 2014.

Daudet, L., and LaBoube, R. (1996). "Shear behavior of self drilllng screws used in low ductility steel." Proc., 13th International Specialty Conference on Cold-Formed Steel Structures, University of Missouri-Rolla, 595–613.

ECCS (1987). "European Recommendations for the Design of Light Gage Steel Members."Brussels, Belgium.

Francka, R. M., and LaBoube, R. A. (2009). "Screwed connection subject to tension pull-out and shear forces."

Haus, A. (2014). Energy Dissipation of Cold-Formed Steel Connections. Virginia Tech Structural and Engineering Materials Report No. CE/VPI-ST-14/02, Blacksburg, Virginia.

Hendawi, S., and Frangopol, D. M. (1994). "System reliability and redudancy in structural design and evaluation." Structural Safety, 16(1), 47-71.

Laboube, R. A., and Sokol, M. A. (2002). "Behavior of screw connections in residential construction." Journal of Structural Engineering, 128(1), 115–118.

Leng, J., Schafer, B. W., and Buonopane, S. G. (2012). "Modeling the seismic response of cold-formed steel framed buildings: model development for the CFS-NEES building." Annual Stability Conference - Structural Stability Research Council, , St. Louis, Missouri.

Lim, J., and Nethercot, D. (2004). "Stiffness prediction for bolted moment-connections between cold-formed steel members." Journal of Constructional Steel Research, 60(1), 85–107.

McKenna, F., Fenves, G. L., Scott, M. H., and Jeremic, B. (2000). "Open System for Earthquake Engineering Simulation (OpenSees)." University of California, Berkeley, CA., Pacific Earthquake Engineering Research Center.

Merwe, P. v. d. (1987). "Development of design criteria for ferritic stainless steel cold-formed structural members and connections " Ph.D. thesis, University of Missouri-Rolla.

Peköz, T. (1990). "Design of cold-formed steel screwed connections." Tenth International Specialty Conference on Cold-formed Steel Structures, Missouri S&T, St. Louis, Missouri, U.S.A.

Serrette, R., and Peyton, D. (2009). "Strength of screw connections in cold-formed steel construction." Journal of Structural Engineering, 135(8), 951–958.

Uang, C., and Sato, A. (2010). "Cyclic Testing and Modeling of Cold-Formed Steel Special Bolted Moment Frame Connections." Journal of Structural Engineering, 136(8), 953–960.

Winter, G. (1956). "Tests on bolted connections in light gage steel." Proceedings of the American Society of Civil Engineers, 101(7), 1381-1391.

Zadanfarrokh, F., and Bryan, E. (1992). "Testing and design of bolted connections in cold-formed steel sections." Eleventh international specialty conference on cold-formed steel structuresUniversity of Missouri-Rolla, St. Louis, Missouri, U.S.A.

Zaharia, R., and Dubina, D. (2006). "Stiffness of joints in bolted connected cold-formed steel trusses." Journal of Constructional Steel Research, 62(3), 240–249.